Available online at www.sciencedirect.com
ScienceDirect
Journal of Pharmaceutical and Biomedical Analysis 47 (2008) 221–229
JOURNAL OF PHARMACEUTICAL AND BIOMEDICAL ANALYSIS
www.elsevier.com/locate/jpba

Non-invasive quantitative assessment of the content of pharmaceutical capsules using transmission Raman spectroscopy

Charlotte Eliasson [a], Neil A. Macleod [a], Linda C. Jayes [b], Fiona C. Clarke [b], Stephen V. Hammond [b], Mark R. Smith [b], Pavel Matousek [a,*]

[a] *Central Laser Facility, Science and Technology Facilities Council, Rutherford Appleton Laboratory, Harwell Science and Innovation Campus, Didcot, Oxfordshire OX11 0QX, United Kingdom*
[b] *Pfizer, Process Analytical Support Group (PASG), Pfizer Ltd., Ramsgate Road, Sandwich, Kent CT13 9NJ, United Kingdom*

Received 15 November 2007; accepted 8 January 2008
Available online 17 January 2008

Abstract

This study demonstrates how transmission Raman spectroscopy can be used in the quantitative, non-invasive probing of the bulk content of production line relevant pharmaceutical products contained within capsules with a strong interfering Raman signal (principally TiO_2). This approach is particularly beneficial in situations where the conventional Raman backscattering method is hampered or fails due to excessive Raman or fluorescence signals emanating from surface layers (capsule or coating) that pollute the much weaker subsurface Raman signals. In these feasibility experiments the interfering surface Raman signal was effectively suppressed, relative to the Raman signal of the internal content, by a factor of 33, in the transmission geometry in comparison with the conventional backscattering Raman approach. In conjunction with the superior bulk probing ability of the transmission Raman geometry, which effectively removes the sub-sampling problem inherent to conventional Raman spectroscopy, and multivariate analysis (principal component analysis (PCA), partial least squares (PLS) and classical least squares (CLS) regression), this provides an analytical tool well suited for rapid control monitoring applications in the pharmaceutical industry. The measured relative root mean square error of prediction (RMSEP) of the concentration of the active pharmaceutical ingredient (API) was 1.2 and 1.8% with 5 and 1 s acquisition times, respectively.

Keywords: Raman; PAT; Pharmaceutical; Transmission; Bulk

1. Introduction

In a number of analytical pharmaceutical applications there is a need for techniques capable of probing capsules or coated tablets *non-invasively* in order to quantitatively monitor the chemical composition in terms of both active pharmaceutical ingredients (API) and other constituents or impurities. For example, in quality control, information is needed rapidly and non-destructively to quantify the presence (or absence) of polymorphs or undesired salt forms of the active ingredient, and unwanted contaminants (including unreacted chemicals from the production and purification stages). The need for such data analysis is emphasized by the Food and Drug Administration's (FDA) Process Analytical Technology (PAT) initiative [1] that requires pharmaceutical manufacturers to ensure the quality of the final product by improved performance monitoring and control.

The need to obtain such information rapidly and non-invasively is dictated by the practical requirements of applications such as quality monitoring on production lines or when quantifying product shelf lifetime. While alternative analytical methods such as X-ray or THz spectroscopy can be used, these approaches are presently relatively expensive [2]. Near infrared (NIR) absorption can also be used non-invasively, but the information obtained is limited in chemical specificity, which restricts its potential application. Raman spectroscopy, on the

* Corresponding author. Tel.: +44 1235 445377; fax: +44 1235 445693.
E-mail address: P.Matousek@rl.ac.uk (P. Matousek).

0731-7085/$ – see front matter.
doi:10.1016/j.jpba.2008.01.013

other hand, possesses exceptionally high chemical specificity and, in conventional backscattering collection mode, has been used for monitoring the composition of pharmaceutical tablets [3–10]. However, with capsules, its applicability to non-invasive probing has been limited to cases where the Raman signal and fluorescence emanating from the capsule shell does not interfere strongly with the Raman signal of the material held within the capsule.

This work builds on recent developments in the area of deep non-invasive probing of diffusely scattering samples using Raman techniques. In particular, two practical methods have been demonstrated to be suitable for the interrogation of pharmaceutical samples, spatially offset Raman spectroscopy (SORS) [11,12] and transmission Raman spectroscopy.

The SORS method is capable of providing resolved spectra of each layer of a stratified sample (e.g. coated tablets or pharmaceutical capsules) and is based on the collection of Raman signals from spatial regions *offset* from the point of illumination on the sample surface. Since the first experimental demonstration of the SORS concept on powders [11], it has been applied in numerous applications including the demonstration of Raman tomography in turbid media and the non-invasive Raman spectroscopy of bones on cadavers by Schulmerich et al. [13–15] and the first observation of the Raman spectrum of a human bone *in vivo* by Matousek et al. [16]. Its potential has also been demonstrated in pharmaceutical applications such as the non-invasive monitoring of counterfeit drugs through packaging by Eliasson and Matousek [17]. Recently, a more sensitive variant, inverse SORS has been demonstrated [18,19]. Research by Eliasson et al. [20] also showed that a moderate suppression of surface signals can be accomplished by defocusing a conventional Raman instrument.

Subsequently [21,22] it has been shown that transmission Raman spectroscopy is particularly effective in probing the *bulk* content of non-absorbing or weakly absorbing pharmaceutical and biological samples at depths well beyond the reach of conventional approaches by removing the bias towards surface layers of the conventional Raman approach (sub-sampling) [21]. In the transmission Raman geometry, the laser beam is incident upon one side of the probed capsule and the Raman light is collected from the *opposite side* (see Fig. 1). This concept can be considered as a special case of SORS with the illumination and collection points situated at extreme displacement. Although the transmission Raman technique was demonstrated in the early days of Raman spectroscopy [23], its benefits for the non-invasive probing of the bulk content of pharmaceutical samples had not been previously recognised. In particular, these include the removal of the so-called sub-sampling problem [21] (over-sensitivity to the surface layers of the probed medium), from which conventional Raman spectroscopy suffers [24], and the effective suppression of fluorescence components emanating from coating or capsule layers [22]. The aforementioned non-invasive Raman methods and their application areas are reviewed in Ref. [25].

This work demonstrates the ability of the transmission Raman method to provide *quantitative information* on the internal composition of capsules where a strong interfering capsule shell

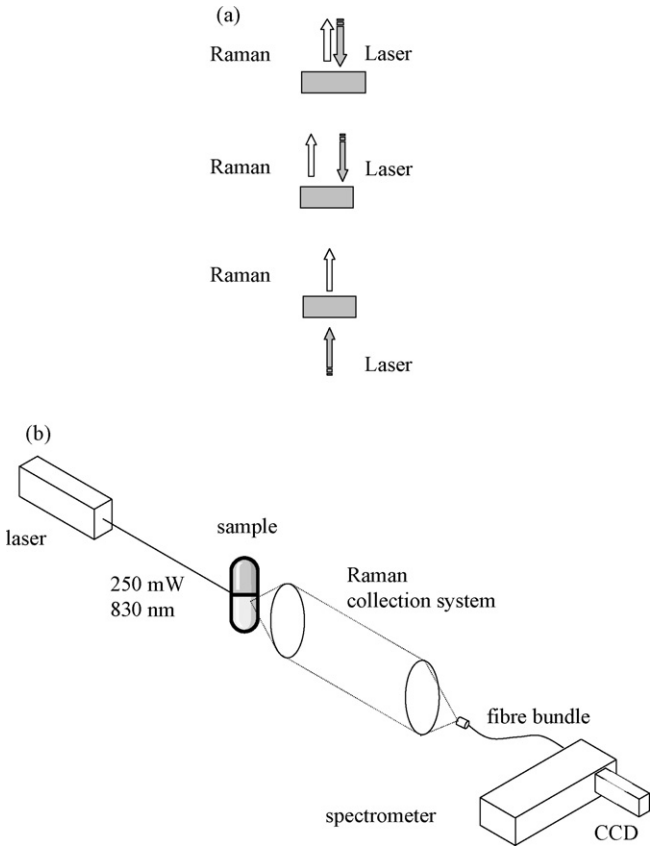

Fig. 1. (a) Illustration of the conventional backscattering Raman, SORS and Raman transmission geometries (from the top to the bottom). (b) Schematic diagram of the experimental layout employing transmission collection geometry.

Raman signal is present in conventional backscattering Raman spectroscopy. The provision of this information is a key prerequisite for the deployment of this method in PAT applications. The general feasibility of the quantification of tablets and capsules using transmission Raman was recently demonstrated by Johansson et al. [26]. This study, using 20 test tablets and an unspecified number of capsules specifically formulated for the trial runs, achieved a relative root mean square error of prediction (RMSEP) of API concentration of 2.2 and 3.6%, respectively, with a 10-s acquisition time. In this work, we applied the transmission Raman technique to an existing drug mass produced and available on the market. The formulations were prepared in a laboratory environment within the relevant production concentration range (Table 1 and Fig. 2). The capsules used possessed strong interfering Raman signal hampering the use of other PAT compatible optical spectroscopy methods such as NIR absorption and conventional Raman spectroscopy for the purposes of non-invasively quantifying the API present in the capsules. The entire sample set contained 150 capsules. The measured relative root mean square error of API prediction was higher than that achieved before 1.2 and 1.8% with 5 and 1 s acquisition times, thus reaching production line relevant accuracy and measurement times. The study demonstrates quantitatively that the transmission geometry suppresses the interfering capsule shell Raman signature (mainly TiO_2), by a factor of 33,

Table 1
Relative concentrations (wt%) of the four ingredients of the laboratory produced batches

Blend (#)	API (wt%)	Mg stearate (wt%)	Pregelatinised starch (wt%)	Lactose (wt%)
1	27.0	0.67	9.5	62.8
2	27.0	1.00	10.0	62.0
3	27.0	1.38	10.5	61.1
4	28.5	0.84	11.0	59.7
5	28.5	1.20	9.0	61.3
6	28.5	0.67	10.0	60.8
7	30.0	1.00	10.5	58.5
8	30.0	1.38	11.0	57.6
9	30.0	0.84	9.0	60.2
10	31.5	1.20	9.5	57.8
11	31.5	0.67	10.5	57.3
12	31.5	1.00	11.0	56.5
13	33.0	1.38	9.0	56.6
14	33.0	0.84	9.5	56.7
15	33.0	1.20	10.0	55.8

and this improves the accuracy and stability of prediction models.

2. Experimental and methods

2.1. Instrumental

The Raman spectra were measured using Raman apparatus described earlier [18] modified to operate in a transmission geometry [21]. The probe beam was generated using a frequency stabilised diode laser operating at 830 nm (Process Instruments, model PI-ECL-830-300-FS). The laser power at the sample was 250 mW and the laser spot diameter was ~3–4 mm. The beam was spectrally purified by removing any residual amplified spontaneous emission components from its spectrum using three 830 nm bandpass filters (Semrock).

Raman light was collected from the opposite side of the sample from the illumination site using a 50-mm diameter lens with a focal length of 60 mm. The scattered light was collimated and passed through a 50-mm diameter holographic notch filter (830 nm, Kaiser Optical Systems Inc.) to suppress the elastically scattered component of light. A second lens, identical to

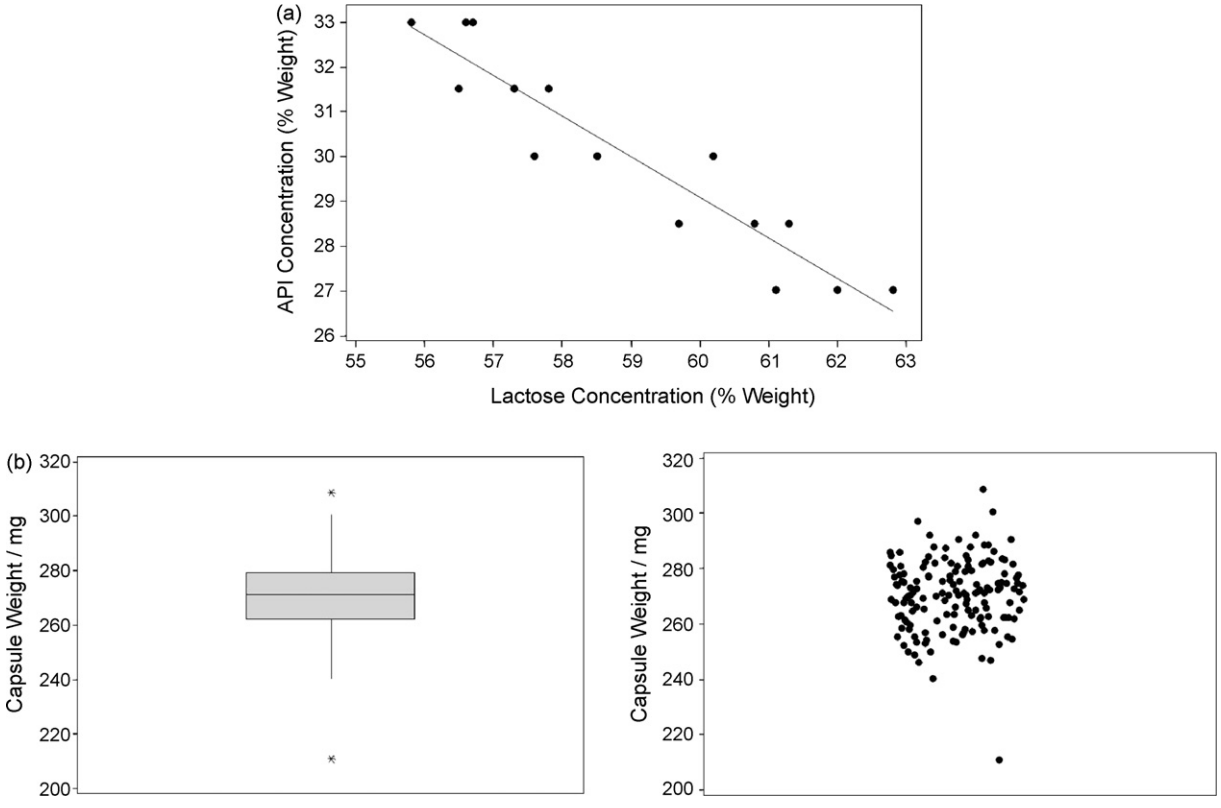

Fig. 2. (a) Plot of API concentration vs. lactose concentration for each laboratory produced batch and (b) scatterplot/boxplot of the total mass of each capsule.

the first, was used to image, with magnification 1:1, the sample collection zone onto the front face of a fibre probe (CeramOptec Industries Inc., numerical aperture = 0.37) made of 22 active optical fibres. The individual fibres were made of silica with a core diameter of 220 μm, a doped silica cladding diameter of 240 μm and a polyimide coating of 265 μm diameter. The fibre bundle length was ∼2 m and at the output end the fibres were arranged into a linear shape [27] oriented vertically and placed in the input image plane of a Kaiser Optical Technologies Holospec 1.8i NIR spectrograph. Raman spectra were collected using a NIR back-illuminated deep-depletion thermoelectrically cooled CCD camera (Andor Technology, DU420A-BR-DD, 1024 × 256 pixels) by binning the entire chip vertically. The spectra are not corrected for the variation of the detection sensitivity across the spectral range. The spectral resolution was estimated to be around 13 cm^{-1}.

The measurements presented in Fig. 3 were obtained using the laboratory instrument under the same conditions as above apart from the laser probe wavelength which was 827 nm and using a lower laser power (50 mW). The comparative Raman measurements using a commercial confocal Raman microscope

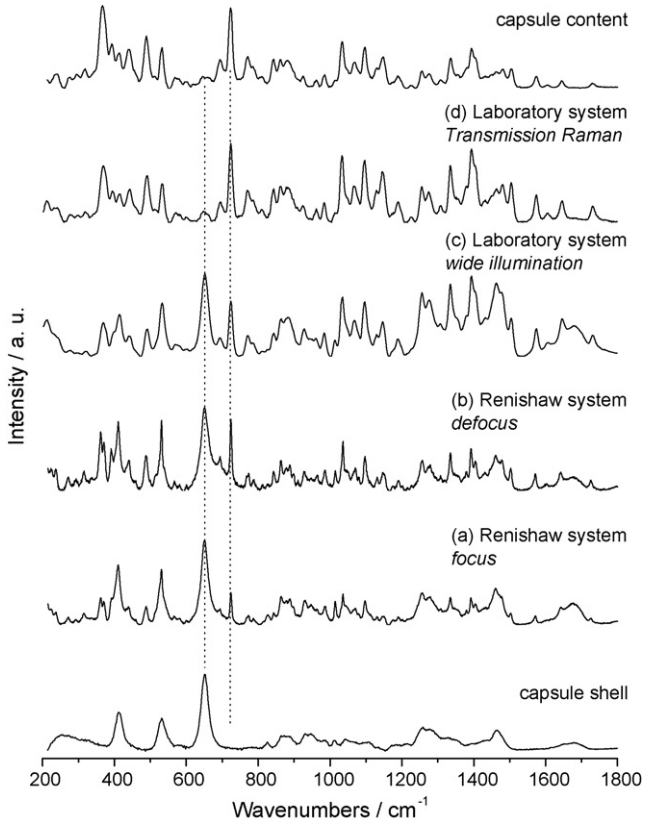

Fig. 3. Non-invasive Raman spectra of capsules. The spectra were obtained using (a) a standard commercial Raman system (Renishaw) in conventional backscattering geometry; (b) the same instrument as used in (a) but in a defocused mode; (c) a wide-area illumination laboratory Raman instrument in the conventional backscattering geometry; (d) the laboratory instrument used in the transmission Raman geometry. The Raman spectra of an empty capsule shell (lowest trace) and the capsule content itself (top trace, the capsule content was transferred into an optical cell) are also shown for comparison. The dashed lines indicate the principal Raman bands of the capsule and of the API.

(Renishaw inVia) were performed with a 20× microscope objective with a probe wavelength of 830 nm and a grating of 1200 lines/mm. The laser power at the sample was 50 mW and acquisition time was 10 s. The spectral resolution was ≤6 cm^{-1}.

2.2. Samples

The accuracy of the concentration of the two dominant constituents (API and lactose) depends on the accuracy of the weighing and blending process as reference potency data was not available for this sample set (see Table 1). For this feasibility study, the samples were laboratory prepared using a PK blender and encapsulated using a hand filler into gelatine capsules. The target weight (274 ± 15%) was based on a target blend weight of 225 mg and a capsule weight of 49 mg (Fig. 2(b)). Given the nature of their composition with only two dominant variable components (API and lactose) a strong concentration correlation was present between these two components (highlighted in Fig. 2(a)).

2.3. Numerical analysis

Spectra were analysed using the MATLAB software package (Version 2006b, Mathworks Inc., Natick, USA) with the PLS toolbox (Version 4.0, Eigenvector Research Inc., Wenatchee, USA) with a combination of in-built and user written scripts.

The pre-processing routine comprised baseline subtraction (with a non-negative spectral constraint [28]), normalisation to unit length (division by the sum of squares of all data points in a spectrum) and mean-centering of the entire dataset. Additional multivariate analysis was performed using The Unscrambler® (Version 9.6, CAMO Software AS, Norway).

The multivariate techniques applied included PCA, PLS regression and CLS regression [29]. The dataset comprised ∼150 individual spectra representing 15 distinct chemical compositions ("blends") with ca. 10 capsules in each blend. Clear outliers (i.e. spectra not representative of the rest of the dataset) were identified visually in the PCA analysis and excluded from further analysis. For the calibration and regression methods, the remaining dataset (containing ∼140 samples) was randomly split into a calibration set (two-thirds) and a prediction set (one-third); this division was repeated 10 times. A model was constructed from each of the calibration sets and applied to the prediction sets; quality of fit was estimated from the RMSEP (Eq. (1)), where Y_{meas} is the reference concentration of the species of interest, Y_{pred} is the predicted concentration and n is the number of points in the prediction set:

$$\mathrm{RMSEP} = \sqrt{\frac{\sum(Y_{meas} - Y_{pred})^2}{n}} \quad (1)$$

For classical least squares analysis, Eq. (2) was solved (for the matrix of pure spectra, S) in terms of the experimental dataset (X) and the concentration matrix (C) using the entire spectral region (200–1800 cm^{-1}):

$$X = CS \quad (2)$$

In the case of PLS regression, the number of latent variables used in the calibration (analogous to the number of principal components in PCA) was assessed by a cross-validation procedure using 10 subsets randomly selected across the calibration set; the optimum number of latent variables was defined as the minimum of the root mean square error of cross-validation (defined in a similar fashion as the RMSEP).

3. Results and discussion

Fig. 3 shows non-invasive Raman spectra of one of the capsules measured using several different approaches. The analysed sample represents the mid-point of the concentration range for both the API and the lactose excipient; the spectra are dominated by these two analytes. Spectrum (a) was obtained using a standard commercial Raman system (Renishaw inVia) in conventional backscattering geometry. The spectrum is strongly contaminated with a Raman spectrum originating from the capsule shell as is evident from comparison with the pure spectrum of the empty capsule shell (Fig. 3, lowest trace). The intensity of the capsule shell signal grossly complicates the quantitative non-invasive analysis of the contents of the capsule using conventional Raman methods. Some reduction, by about a factor of 2, can be accomplished by defocusing the Raman instrument [20] although the resulting interference is still substantial (Fig. 3(b)). A comparable conventional backscattering Raman spectrum was also obtained using a wide-area illumination laboratory Raman instrument (Fig. 3(c)) producing a spectrum similar to that obtained using the defocused confocal Raman microscope.

A dramatic reduction of the Raman signal of the capsule shell relative to that of the capsule interior, by a factor of 33, was accomplished using the laboratory system operated in the *transmission Raman geometry* (Fig. 3(d)). The absolute Raman signal of the capsule interior diminished *only* by a factor of 18 enabling relatively short acquisition times to be maintained. The capsule shell Raman signature is dominated by the Raman signal of TiO_2 (anatase) [30] which contaminates the conventional Raman spectrum of the formulation with undesired noise, thus diminishing its prediction sensitivity and accuracy. Such layers are also known to present a considerable challenge to NIR absorption spectroscopy. Its strong reduction accomplished with the transmission Raman approach is highly beneficial to the stability and accuracy of prediction models.

Typical spectra used in the multivariate analysis are shown in Fig. 4. The results of PCA on the complete dataset with an acquisition time of 5 s are shown in Fig. 5; similar results were obtained using a 1-s accumulation time. Each spectrum was baseline corrected, normalised to unit length and mean-centered before analysis. The eigenvalues (Fig. 5(a)) indicate the presence of two or three significant principal components, in broad agreement with the designed concentrations (major components API (∼30%) and lactose (∼60%) and minor components starch (∼9%) and magnesium stearate (∼1%)) and the fact that the concentrations of lactose and API are correlated. The first principal loading vector/eigenvector (Fig. 5(b)) can be understood (from reference spectra of the pure constituents) as a combination of the spectrum of the API (positive peaks) and that of lactose (negative peaks). The inverse correlation between the main constituents is a result of the experimental design of the sample composition (see Fig. 2(a)).

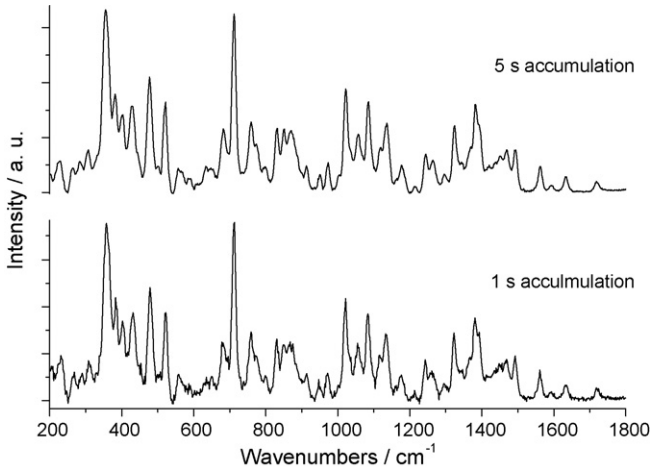

Fig. 4. Typical capsule transmission Raman spectra, with acquisition times of 1 and 5 s, as used in the multivariate analysis. The spectra have been corrected for background fluorescence.

Plots of the scores of each spectrum on the first principal component versus API or lactose concentration (Fig. 5(c) and (d)) show a clear linear correlation; the constituent capsules of each individual blend group form relatively well-defined clusters. Data points outlying from the general behaviour can be readily identified (points 20, 40 and 71–80). The tight cluster of tablets of blend 8 (samples 72–80) and its deviation from a linear correlation indicated an error in the production or labelling of this particular blend; a similar behaviour was found in the data recorded with 1 s accumulation time. A subsequent HPLC analysis confirmed that this blend indeed had a substantially lower quantity of API (25.3%) relative to the target concentration (30.0%). Remarkably, this value was correctly indicated by the transmission Raman measurement (see Fig. 5) despite being well outside of the concentration range of the remaining samples emphasizing the robustness of the method. HPLC analysis of two other, randomly selected, blends gave API concentrations in agreement with the target concentrations. The remaining outliers (20, 40 and 71) can be traced to random variations of the measurement parameters or the presence of other errors; a similar number of outliers (comprising different sample spectra) were found in the 1 s dataset. All outliers were excluded from further analysis.

Figs. 6 and 7 show the predicted versus measured concentrations of lactose and API from PLS and CLS regression, respectively, of the dataset collected with 5 s accumulation time; similar results were obtained using the 1 s dataset. Values of the RMSEP are given in Table 2 for API and lactose. The entire spectral range (200–1800 cm^{-1}) was used in the calibration; typically 1–2 latent variables were required to model the API concentration while 2–3 were required for the lactose excipient.

Both calibration methods provide prediction errors (RMSEP) of the order of 1% of the absolute concentration. PLS regression gives a lower value of RMSEP (0.4% absolute prediction

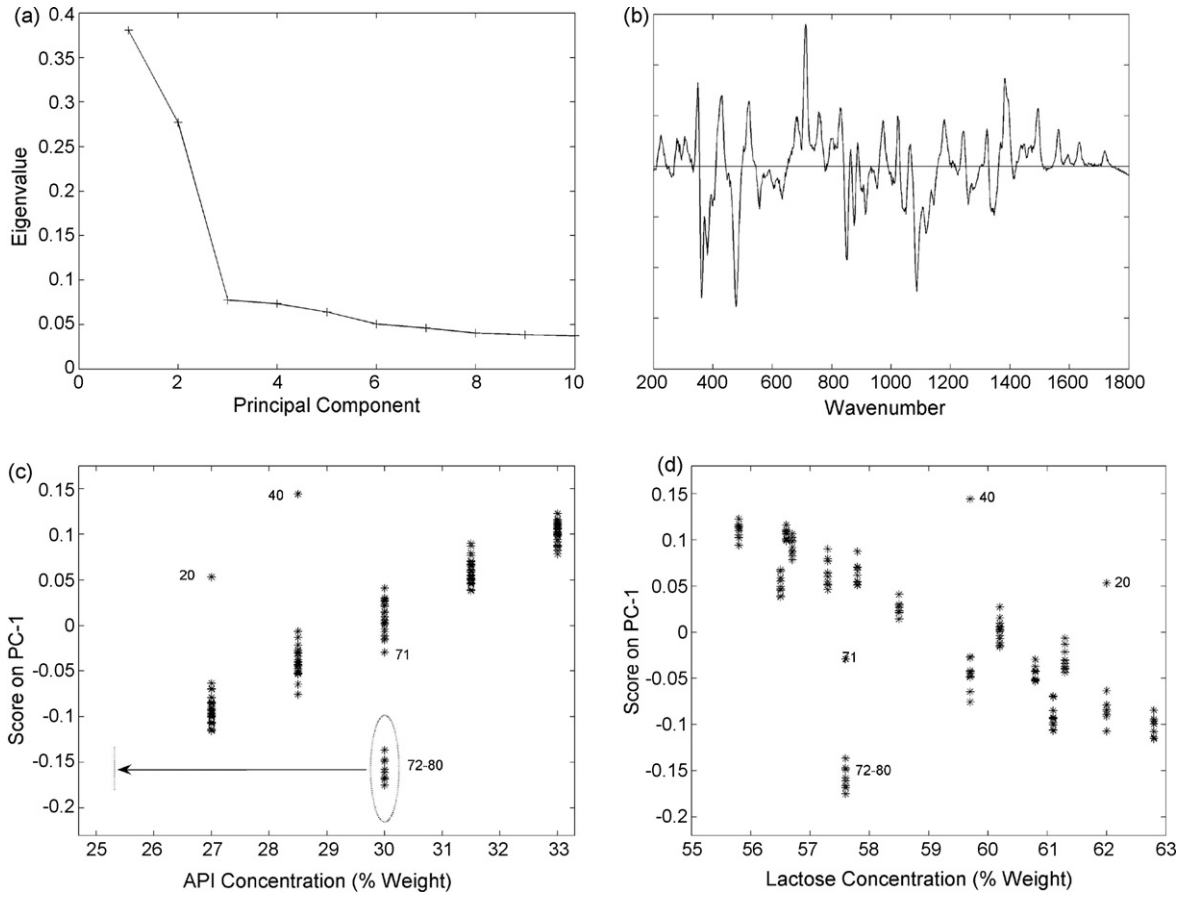

Fig. 5. Principal components analysis (PCA) of the API dataset. Spectra were baseline corrected, normalised to unit length and mean-centered. (a) Plot of eigenvalues vs. number of principal components, (b) first principal eigenvector (loading vector); "positive" peaks correspond to API bands, "negative" peaks to lactose, (c) plot of score of each spectrum on the first principal component vs. API concentration (a subsequent HPLC analysis confirmed that samples 72–80 had a substantially lower quantity (25.3%) of API than designed (indicated by the dotted line) in good agreement with an extrapolation based on the remaining samples) and (d) plot of score of each spectrum on the first principal component vs. lactose concentration.

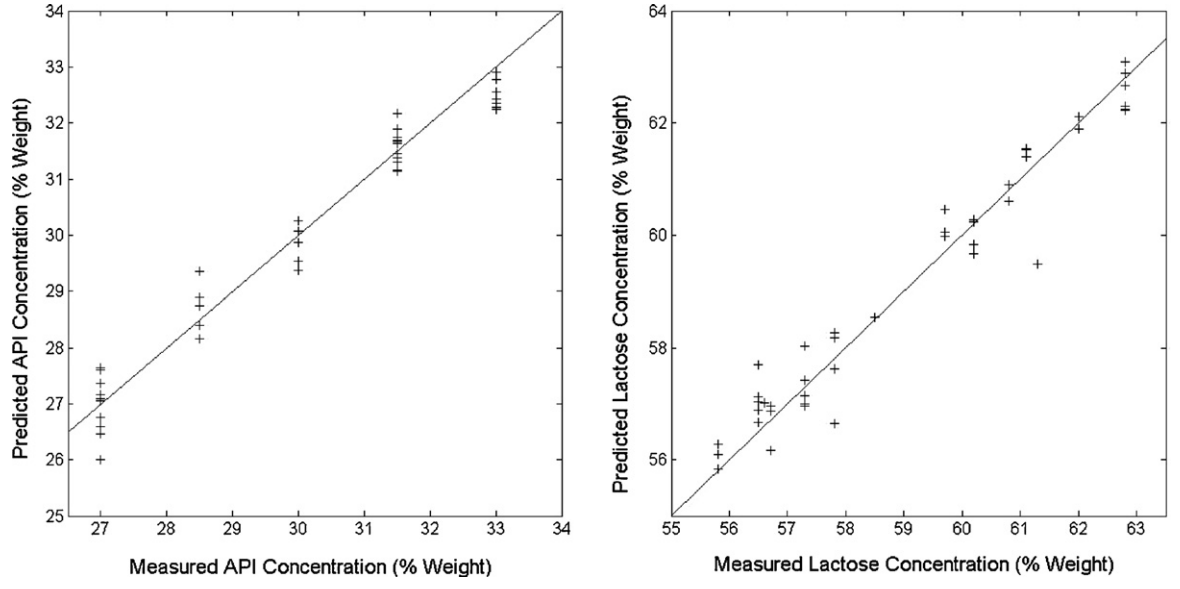

Fig. 6. Partial least squares (PLS) calibration of the API dataset (5 s accumulation time). Spectra were baseline corrected, normalised to unit length and mean-centered. The dataset was randomly split into a calibration set (two-thirds) and a prediction set (one-third); obvious outliers from the PCA analysis were excluded from the analysis. (a) Predicted vs. measured API concentration of the prediction set, the straight line represents the 45° diagonal and (b) predicted vs. measured lactose concentration of the prediction set. The straight line represents the 45° diagonal.

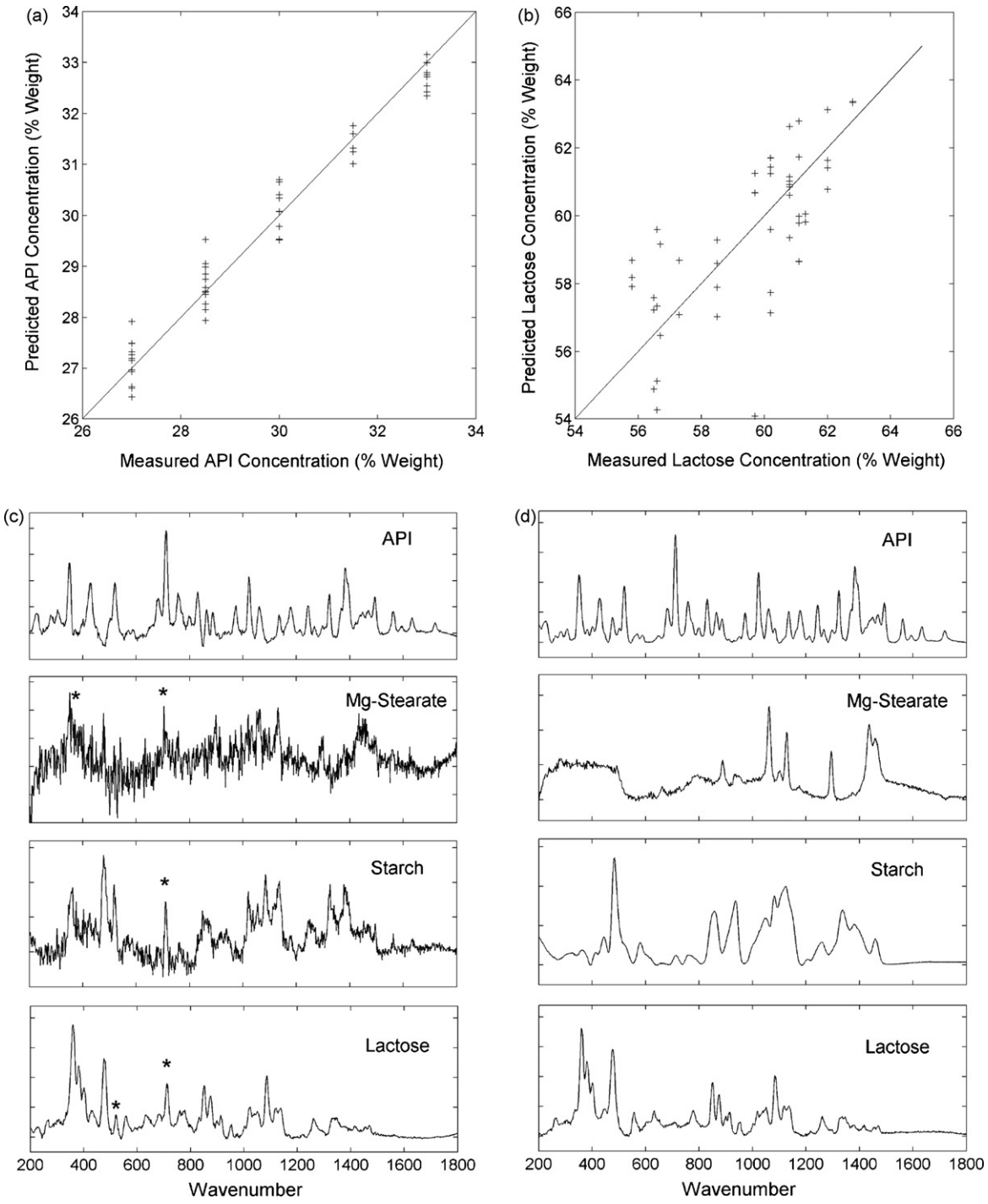

Fig. 7. Classical least squares (CLS) calibration of the API dataset (5 s accumulation time). Spectra were baseline corrected, normalised to unit length and mean-centered. The dataset was randomly split into a calibration set (two-thirds) and a prediction set (one-third); obvious outliers from the PCA analysis were excluded from the analysis. (a) Predicted vs. measured API concentration of the prediction set, the straight line represents the 45° diagonal. (b) Predicted vs. measured lactose concentration of the prediction set, the straight line represents the 45° diagonal. (c) Computed component spectra of the four constituents from the calibration set, asterisks indicate bands of API and lactose which appear in the spectra of the other components and (d) reference Raman spectra of the pure components.

error corresponding to 1.2% relative prediction error) than CLS. Comparison between the spectra computed from CLS and the reference spectra of the pure ingredients (Fig. 7(c) and (d)) show significant spectral overlap for all species in the 400–1500 cm^{-1} region which can result in inaccuracies in the CLS method. The spectra computed from the concentration data (Fig. 7(c)) show a number of bands of lactose and API which appear in, and pollute, the spectra of the other components which adversely affects the predicted concentrations. In particular, the API has a rich vibrational spectrum which has significant overlap with each of the other ingredients. Furthermore, the concentrations of the two main ingredients are correlated which will also adversely

Table 2
Root mean square errors of prediction (RMSEP) for API and lactose for data recorded at 1 and 5 s accumulation time

	API RMSEP (wt%)	Lactose RMSEP (wt%)
1-s accumulation		
CLS	0.77	0.95
PLS	0.59	0.69
5-s accumulation		
CLS	0.49	1.69
PLS	0.40	0.55

Outliers have been excluded. The data was baseline corrected, normalised to unit length and mean-centered. Errors are an average over 10 randomly selected runs.

influence the CLS calibration. The substantial improvement in prediction accuracy for the PLS method over the CLS method for lactose appears to derive from a more complex model incorporating additional latent variables (3) which, to some degree, breaks the correlation between the concentrations.

An additional note of caution should also be addressed here; although the transmission geometry reduces the relative influence of the Raman signal of the capsule, it does not completely eliminate it. Therefore a CLS-based calibration should include the concentration of the capsule for completeness. However, this concentration is essentially unknowable as is the variation in capsule thickness (and hence concentration) between capsules; for these reasons a PLS-based calibration, where any variation is included as part of the model, may be preferred.

This feasibility study has demonstrated the potential of Raman spectroscopy, in transmission mode, for the quantitative analysis of pharmaceutical samples under the presence of strong interfering Raman signal of capsule shell. The overall accuracy of prediction (∼1% of the measured concentrations) is comparable with those derived from other non-invasive techniques, i.e. NIR absorption, for which a relative prediction error of 1–2% would typically be considered acceptable in a routine manufacturing environment. Further improvements in prediction accuracy and stability/robustness may be expected using a variety of approaches including the selection of spectral regions particularly sensitive to each analyte [31–33] and an expanded range of samples spanning all potential concentrations and with minimal correlation between the ingredients.

4. Conclusions

This study has demonstrated experimentally the feasibility of quantifying the content of pharmaceutical capsules non-invasively using transmission Raman spectroscopy. Substantial reductions, relative to conventional backscattering Raman, in both Raman and fluorescence signals from the capsule shell allow the spectrum of the internal, bulk, components to be obtained. This property, in combination with the superb chemical specificity of Raman spectroscopy, rapid data acquisition and ease of deployment makes the transmission Raman concept particularly well suited for the rapid analysis of pharmaceutical capsules and tablets. Multivariate techniques (including PCA and PLS calibration) allow atypical samples (outliers) to be detected and a model constructed to predict the bulk properties of the capsule. The ability to use defocused beams with transmission Raman spectroscopy (in contrast with conventional Raman microscopy) dramatically reduces the risk of sample photo-damage. For the laser sources used here (830 nm) only near-infrared photo-active samples would be susceptible to damage.

Acknowledgements

We wish to thank Dr. Darren Andrews and Dr. Tim Bestwick of CLIK Knowledge Transfer and Mrs. Sue Tavender, Professor Tony Parker and Professor Mike Dunne of the Science and Technology Facilities Council for their support of this work. We also wish to acknowledge the financial contribution of the EPSRC (EP/D037662/1), CLIK Knowledge Transfer, NESTA and the Rainbow Seed Fund for enabling this study.

References

[1] http://www.fda.gov/Cder/OPS/PAT.htm.
[2] C.J. Strachan, P.F. Taday, D.A. Newnham, K.C. Gordon, J.A. Zeitler, M. Pepper, T. Rades, J. Pharm. Sci. 94 (2005) 837–846.
[3] A.C. Williams, V.B. Cooper, L. Thomas, L.J. Griffith, C.R. Petts, S.W. Booth, Int. J. Pharm. 275 (2004) 29–39.
[4] C. Wang, T.J. Vickers, C.K. Mann, J. Pharm. Biomed. Anal. 16 (1997) 87–94.
[5] M. Dyrby, S.B. Engelsen, L. Norgaard, M. Bruhn, L. Lundsberg-Nielsen, Appl. Spectrosc. 56 (2002) 579–585.
[6] J. Johansson, S. Pettersson, S. Folestad, J. Pharm. Biomed. Anal. 39 (2005) 510–516.
[7] S.E.J. Bell, D.T. Burns, A.C. Dennis, L.J. Matchett, J.S. Speers, Analyst 125 (2000) 1811–1815.
[8] D.S. Hausman, R.T. Cambron, A. Sakr, Int. J. Pharm. 299 (2005) 19–33.
[9] R. Szostak, S. Mazurek, Analyst 127 (2002) 144–148.
[10] J. Breitenbach, W. Schrof, J. Neumann, Pharm. Res. 16 (1999) 1109–1113.
[11] P. Matousek, I.P. Clark, E.R.C. Draper, M.D. Morris, A.E. Goodship, N. Everall, M. Towrie, W.F. Finney, A.W. Parker, Appl. Spectrosc. 59 (2005) 393–400.
[12] P. Matousek, M.D. Morris, N. Everall, I.P. Clark, M. Towrie, E. Draper, A. Goodship, A.W. Parker, Appl. Spectrosc. 59 (2005) 1485–1492.
[13] M.V. Schulmerich, W.F. Finney, R.A. Fredricks, M.D. Morris, Appl. Spectrosc. 60 (2006) 109–114.
[14] M.V. Schulmerich, W.F. Finney, V. Popescu, M.D. Morris, T.M. Vanasse, S.A. Goldstein, in: A. Mahadevan-Jansen, W.H. Petrich (Eds.), Proceedings of the SPIE 6093 Biomedical Vibrational Spectroscopy III: Advances in Research and Industry, February 27, 2006, p. 60930O.
[15] M.V. Schulmerich, K.A. Dooley, T.M. Vanasse, S.A. Goldstein, M.D. Morris, Appl. Spectrosc. 61 (2007) 671–678.
[16] P. Matousek, E.R.C. Draper, A.E. Goodship, I.P. Clark, K.L. Ronayne, A.W. Parker, Appl. Spectrosc. 60 (2006) 758–763.
[17] C. Eliasson, P. Matousek, Anal. Chem. 79 (2007) 1696–1701.
[18] P. Matousek, Appl. Spectrosc. 60 (2006) 1341–1347.
[19] M.V. Schulmerich, K.A. Dooley, M.D. Morris, T.M. Vanasse, S.A. Goldstein, J. Biomed. Opt. 11 (2006) 060502.
[20] C. Eliasson, M. Claybourn, P. Matousek, Appl. Spectrosc. 61 (2007) 1123–1127.
[21] P. Matousek, A.W. Parker, Appl. Spectrosc. 60 (2006) 1353–1357.
[22] P. Matousek, A.W. Parker, J. Raman Spectrosc. 38 (2007) 563–567.
[23] B. Schrader, G. Bergmann, Zeitschrift fur Analytische Chemie Fresenius 225 (1967) 230–247.
[24] J. Johansson, S. Pettersson, S. Folestad, J. Pharm. Biomed. 39 (2005) 510–516.
[25] P. Matousek, Chem. Soc. Rev. 36 (2007) 1292–1304.

[26] J. Johansson, A. Sparen, O. Svensson, S. Folestad, M. Claybourn, Appl. Spectrosc. 61 (2007) 1211–1218.
[27] J.Y. Ma, D. Ben-Amotz, Appl. Spectrosc. 51 (1997) 1845–1848.
[28] C.A. Lieber, A. Mahadevan-Jansen, Appl. Spectrosc. 57 (2003) 1363–1367.
[29] D.M. Haaland, E.V. Thomas, Anal. Chem. 60 (1988) 1193–1202.
[30] I.M. Clegg, N.J. Everall, B. King, H. Melvin, C. Norton, Appl. Spectrosc. 55 (2001) 1138–1150.
[31] M.R. Smith, R.D. Jee, A.C. Moffat, D.R. Rees, N.W. Broad, Analyst 128 (2003) 1312–1319.
[32] L. Norgaard, A. Saudland, J. Wagner, J.P. Nielsen, L. Munck, S.B. Engelsen, Appl. Spectrosc. 54 (2000) 413–419.
[33] J.H. Jiang, R.J. Berry, H.W. Siesler, Y. Ozaki, Anal. Chem. 74 (2002) 3555–3565.